The Foresighted Driver: Future ADAS Based on Generalized Predictive Risk Estimation

Julian Eggert [*] **Stefan Klingelschmitt** [**] **Florian Damerow** [**]

[*] *Honda Research Institute (HRI) Europe, Carl-Legien-Str. 30, 63073 Offenbach, Germany (e-mail: julian.eggert@honda-ri.de)*
[**] *Control Methods and Robotics Lab, Technical University of Darmstadt, 64283 Darmstadt, Germany (e-mail: [stefan.klingelschmitt, florian.damerow]@rmr.tu-darmstadt.de)*

Topics: Driver Behavior Modeling, Vehicle Dynamics Control and Autonomous Driving, Active Safety testing Methods and Tools

Abstract: Separably developed functionality as well as increasing situation complexity poses problems for building, testing, and validating future Advanced Driving Assistance Systems (ADAS). These will have to deal with situations in which several current ADAS domains interplay. We argue that a generalized estimation of the future ADAS functions' benefit is required for efficient testing and evaluations, and propose a quantification based on an estimation of the predicted risk. The approach can be applied to several different types of risks and to such diverse scenarios as longitudinal driving, intersection crossing and lane changes with several traffic participants. Resulting trajectories exhibit a proactive, "foresighted" driver behavior which smoothly avoids potential future risks.

1. INTRODUCTION

We are currently seeing a phase of increased Advanced Driving Assistance Systems (ADAS) functionality for driver support, comprising forward collision warning (FCW), autonomous emergency braking (AEB), traffic jam assist (TJA), cross traffic assist (CTA) and several more. Common to all these is that they have been developed and validated for a specific narrow working domain in terms of context evaluation, operation range and even interfaces and interaction concepts. Future Adaptive Driver Assistance Systems applicable to more complex situations, say, a mixed longitudinal/lateral behavior situation while overtaking on the highway in the presence of multiple other traffic participants, or a multilane crossing with combined frontal and lateral urban traffic, will require (i) a generalization resp. seamless interplay of the concepts used for the existing, specialized ADAS functions, (ii) an extended analysis of the drivers context in terms of larger numbers of interacting traffic participants and road structure information, (iii) a larger prediction horizon for the dynamics of the ego-vehicle and the other traffic participants and (iv) a quantification and validation of the operating system.

On one side, an extended analysis of the drivers context implies capabilities for the automatic interpretation of the current driving situation, as well as the estimation of the consequences a situation interpretation has on the ego-vehicle's behavior options. On the other side, a validation of the future ADAS functions requires new approaches to deal with the combinatorial variety of parameter settings. The rising situation complexity, together with the sparsity of events (e.g. one fatal accident per 127 million driven km, Shladover (2009)) that can be used for a statistical validation of a system in real world operation, leads to prohibitively high testing costs. Common to the extended context analysis and the system validation is that both need a quantification in terms of usefulness for the drivers purpose.

In this work we propose to model the usefulness as a combination between risk and utility. Utility can be measured in a straightforward way as e.g. the time and money required to travel from A to B. On the other hand, general risk is considered as the probability of something happening multiplied by the resulting cost if it does. Since standard risk indicators like Time-to-Contact (TTC) are not sufficient for dealing arbitrary situations, we take an approach for the quantification of general driving risks according to Eggert (2014) and show how it can be used to implement a risk and utility based behavior planning or driver behavior support, for situations of incremental complexity.

The approach comprises the following steps:

- A classification of the current scenario into situation hypotheses as perceived from the ego-vehicle perspective, based on context information and the spatiotemporal pattern of interactions between traffic participants.
- A selection step based on the situation hypotheses and their estimated associated empirical risks. The result is a subset of situation hypotheses considered relevant for the ego-car behavior that apply to the current scenario.
- A prediction step during which we extrapolate the future development of each of the selected situation hypotheses resp. the states of the traffic participants.

- For each situation hypothesis and for a variety of own intended trajectories, an estimation of the future predicted risk and utility. For each situation we then get a risk landscape (*risk map*) which we can use for detecting the future points of high criticality.
- The planning of appropriate ego-car behavior options which cover the space of possible behaviors avoiding points of maximal risk in the risk landscape.
- The evaluation (for ADAS support and warning functions) or selection (for autonomous driving functions) of the most appropriate ego-car behavior according to their overall expected risk and utility.

From a systems perspective, it has been postulated that most ADAS functions rely on the 4 steps of object assessment, situation assessment, risk assessment and decision making, Hall and Llinas (1997). These steps are sufficiently general to be matched to a large variety of systems including the one presented in this paper. However, several components of these 4 steps, as it is the case for appropriate risk metrics and situation prediction technologies, are subject of current research.

In Lefèvre et al. (2013), a difference is made between intentions and expectations of the driver, and risk is assessed by detecting conflicts between the two. It is argued that such an approach is supported by the fact that a large number of accidents is caused by driver errors, see e.g. TRACE project (2008). However, such a model does provide rather a kind of alertness level for an observing driver than a quantifiable risk measure for the ego-vehicle.

In general, *risk estimation* approaches can be divided into 2 major groups. On one side, holistic systems incorporate context information to directly identify the criticality of a traffic situation, extrapolating from previously recorded data or using criticality rules and indicators. Learning systems, knowledge-based systems and systems that rely on risk indicators like TTC (see e.g. van der Horst (1991); Hillenbrand et al. (2006)) fall into this group. Systems that learn from empirical data have been successfully trained to identify potentially dangerous situations based on databases with accident recordings, see Chinea and Parent (2007); Salim et al. (2007). One issue here is that *representative* data is not available to a sufficient extent, neither from real recordings nor from simulations; another drawback is that scalability from simple to more complex situation patterns is difficult.

This first group of approaches involves a strong predictive component, since risk always means *hypothetical future risk*. In the learning approaches, the prediction is implicit, and comes from the mapping between the vehicle states to an accident event or criticality measure some time after. Similary, knowledge and indicator-based systems detect criticality based on sets of heuristics, where a prediction is implicitly comprised in the designed rules and risk indicators, so that e.g. a too high speed before the crossing may imply a risk when the car reaches the intersection.

In the second group, risk estimation approaches are based on internal simulations for predicting the future time course of the entities in the environment. The risk is then calculated as a function of the future states, see e.g. Althoff et al. (2009); Käfer et al. (2010); Rodemerk et al. (2012). Popular are trajectory estimation methods, which use different motion models to predict the possible future states and then check trajectories for mutual collisions. The degree of model complexity of the prediction models varies, ranging from motion models without constraints up to models which incorporate different driving maneuvers and the current road layout, see e.g. Lefèvre et al. (2014) for a review. To consider the uncertainty spread of possible future trajectories, sampling-based methods are frequently used. Popular behavior planning based on grid and potential-field-based context representations also fall into this group.

In this paper, the contribution to active safety systems concentrates on a system with the steps of understanding the current driving situation, efficiently predicting the behavior of the relevant entities in the environment, estimating the level of expected future danger that the situation poses, and planning the most appropriate driving behavior which should be taken in order to lower the danger. Our approach is based on a rigorous foundation of probabilistic risk for traffic scenarios and provides a formal justification why both approaches - holistic risk estimation on one side and detailed state prediction with risk evaluation as function of predicted states on the other side - are needed for an efficient, general-purpose risk estimation.

2. SITUATION-BASED RISK EVALUATION AND BEHAVIOR PLANNING

Figure 1 shows a rough overview of the different components of the general approach for behavior generation, based on risk considerations. Starting from the left-hand side, knowledge $\mathbf{x}_t$ about the scene at time t is acquired using sensor measurements. Since the scene may be composed of several entities (e.g. different traffic participants, infrastructure elements, etc.) with state vectors $\mathbf{x}_t^i$ (ego car state $\mathbf{x}_t^0$), we write $\mathbf{x}_t := \{\mathbf{x}_t^0, \mathbf{x}_t^1, ..., \mathbf{x}_t^n\}$. Using discrete time step indices $t, t+1, ..., t+s$ (time step size Δt), we additionally introduce state vector sequences

$$\mathbf{x}_{t:t+s} := \{\mathbf{x}_t, ..., \mathbf{x}_{t+s}\} \tag{1}$$

which describe e.g. the states of the scene from t (now) until a time $t+s$ (s into the future).

The overall target of the system is to compute a behavior in form of a trajectory over the ego-car states $\mathbf{x}_{t:t+s}^0$ which minimize an expected/predicted risk. Since risk is the probability that a disruptive event (e.g., an accident) happens, multiplied by the cost resp. the damage if it does, we define future risk [1] at $t+s$ as the cost expectation value

$$r(t+s, \mathbf{x}_t) = \int c_{t+s} P(c_{t+s}|\mathbf{x}_t) \, dc_{t+s} \tag{2}$$

where $P(c_{t+s}|\mathbf{x}_t)$ is the probability of a damage c_{t+s} which happens at $t+s$, if we know the states $\mathbf{x}_t$ of the current scene.

An all-situation risk prediction is computationally infeasible, therefore we partition the prediction space into different prototypical situation classes. A situation combines a small subset of interacting entities (usually car-car or car-infrastructure pairs) with a prototypical spatiotemporal behavior pattern $\hat{\mathbf{x}}_{t+1:t+s}$ (with $\hat{\mathbf{x}}_t = \mathbf{x}_t$), like the ego-car braking to give another car right-of-way at an intersection.

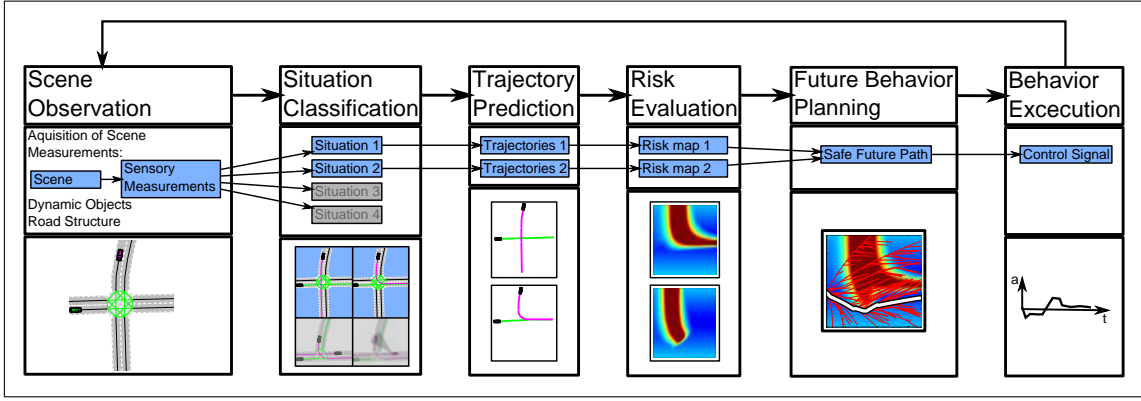[1] To be precise, this is the risk *density* over time.

Fig. 1. General approach for situation based risk evaluation and behavior planning.

This results in situation-specific state vector sequences which depend on the situation hypotheses h_t, so that we get

$$P(c_{t+s}|\mathbf{x}_t) = \sum_{h_t} P(c_{t+s}|\mathbf{x}_t, h_t) P(h_t|\mathbf{x}_t) \qquad . \qquad (3)$$

The situation hypotheses probabilities $P(h_t|\mathbf{x}_t)$ are calculated at t from the evidence $\mathbf{x}_t$ and are valid during the prediction interval $[t, t+s]$, until their calculation is renewed. In Fig. 1, second box from left, the situation classification component is shown.

The situation-dependent damage probability from (3) can be expanded to

$$P(c_{t+s}|\mathbf{x}_t, h_t) := \int d\mathbf{x}_{t+s} \dots \int d\mathbf{x}_{t+1} \qquad (4)$$

$$\sum_{e_{t+s}} P(c_{t+s}|e_{t+s}, \mathbf{x}_{t+s}) P(e_{t+s}|\mathbf{x}_{t:t+s}) P(\mathbf{x}_{t+1:t+s}|\mathbf{x}_t, h_t)$$

i.e., a combination of (i) a damage probability $P(c_{t+s}|...)$ given that an event e_{t+s} happens at $t+s$ and the states at the event time are known, (ii) a future event triggering probability $P(e_{t+s}|...)$ which depends on the predicted state sequence $\mathbf{x}_{t:t+s}$, and (iii) a prediction probability $P(\mathbf{x}_{t+1:t+s}|...)$ of the state vector sequences $\mathbf{x}_{t+1:t+s}$ for each situation hypothesis h_t, if we start with states $\mathbf{x}_t$.

The discrete variable e_{t+s} describes the event class such as e.g. car-to-car, car-to-pedestrian or car-to-infrastructure collisions or control loss at drivability limits. For each of them, a specific damage probability $P(c_{t+s}|e_{t+s}, \mathbf{x}_{t+s})$ is used, e.g. car-to-car accidents are modeled using a partially inelastic collision approach. In addition, $e_{t+s} = 0$ indicates no event, in this case the costs are given by efficiency, utility and comfort considerations.

The event triggering probability $P(e_{t+s}|\mathbf{x}_{t:t+s})$ can be calculated using a so-called *survival function* as used in this paper (see Eggert (2014)), or by checking physical collision by coincident spatial occupancy (Schreier et al. (2014)). What remains to be calculated is the situation-dependent state prediction $P(\mathbf{x}_{t+1:t+s}|\mathbf{x}_t, h_t)$. A standard way is to use (expensive) stochastic sampling methods in combination with appropriate propagation probabilities $P(\mathbf{x}_{t'+1}|\mathbf{x}_{t'}, h_t)$ from one timestep to the next. However, to reduce the complexity of the integrals in (4) yet appropriately capture the growing prediction uncertainty over time, we approximate the probabistic state vector

sequence by its situation-specific prototypical state vector sequence $\hat{\mathbf{x}}_{t+1:t+s}$,

$$P(\mathbf{x}_{t+1:t+s}|\mathbf{x}_t, h_t) \sim \delta(\mathbf{x}_{t+1:t+s} - \hat{\mathbf{x}}_{t+1:t+s}(\mathbf{x}_t, h_t)) \quad (5)$$

and model the growing uncertainty in the event triggering probability by incorporating explicitly the prediction time s to get $P(e_{t+s}|\mathbf{x}_{t:t+s}, s)$. As a second approximation, for simplification [2] we introduce a deterministic damage calculation for fixed known states $\mathbf{x}_{t+s}$,

$$P(c_{t+s}|e_{t+s}, \mathbf{x}_{t+s}) \sim \delta(c_{t+s} - \hat{c}_{t+s}(e_{t+s}, \mathbf{x}_{t+s})) \quad (6)$$

Taking eqs. (2), (3) and (4) and inserting eqs. (5) and (6), results in the final risk estimation formula

$$r(t+s, \mathbf{x}_t) = \sum_{h_t} r(t+s, \mathbf{x}_t, h_t) P(h_t|\mathbf{x}_t) \quad (7)$$

with the situation-dependent risk

$$r(t+s, \mathbf{x}_t, h_t) \sim \sum_{e_{t+s}} \hat{c}_{t+s}(e_{t+s}, \hat{\mathbf{x}}_{t+s}(\mathbf{x}_t, h_t))$$
$$P(e_{t+s}|\hat{\mathbf{x}}_{t+1:t+s}(\mathbf{x}_t, h_t), s) \quad . \quad (8)$$

The risk calculation therefore contains a damage cost calculation according to $\hat{c}_{t+s}$ for critical events, a future event triggering probability $P(e_{t+s}|...)$ which depends on the predicted prototypical state sequence $\hat{\mathbf{x}}_{t:t+s}(\mathbf{x}_t, h_t)$, and a situation hypothesis probability $P(h_t|\mathbf{x}_t)$.

The prediction of future states $\hat{\mathbf{x}}_{t:t+s}(\mathbf{x}_t, h_t)$ is achieved by a deterministic interactive agent model according to Eggert et al. (2015), however, arbitrary other models with a sufficient behavior complexity can be used here. In Fig. 1, third box, predicted trajectory pairs are shown for 2 different situation hypotheses. In the 4th box, the risk is calculated according to (7) for different ego-car behavior options, yielding so-called *risk maps*. In the 5th box, behaviors are planned by searching for the best trajectories in terms of overall cost. Finally, the 6th box shows the selected behavior execution.

The situation classification and its benefits are explained in section 3. The detailed risk evaluation, behavior planning and execution are extended in section 4. The result is a behavior estimation based on generalized predictive risk estimation.

---

[2] This is however not necessary so that a full probabilistic treatment of the damage can be easily incorporated back again.
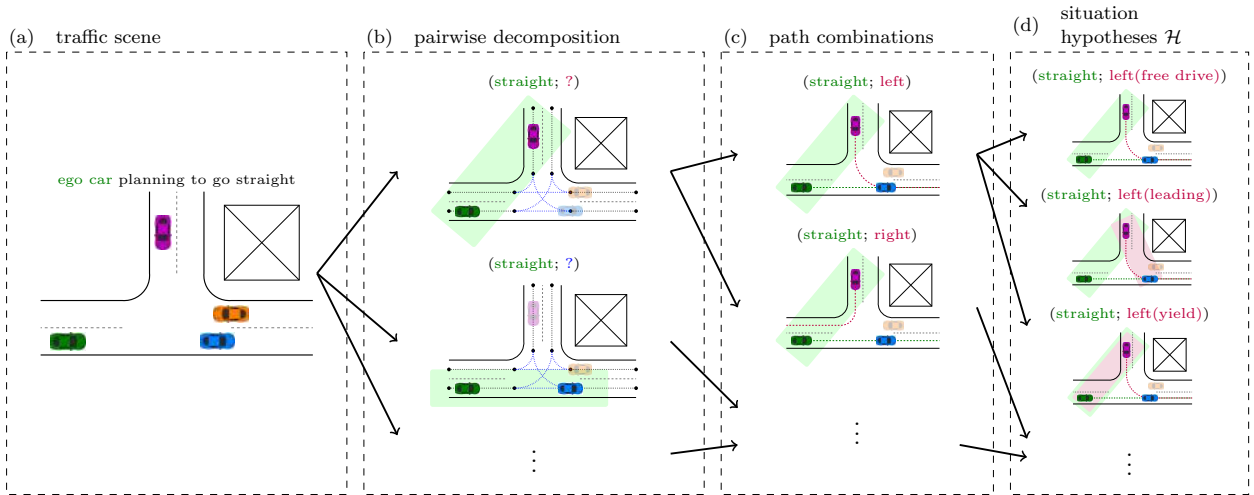
Fig. 2. Hypotheses generation, starting from a complex traffic scene (a). In (b), the scene is decomposed into interacting entity pairs (green boxes), containing the ego-vehicle. In (c), possible path combinations are considered. In (d), for each of the affecting vehicle's potential dynamic behavior patterns a situation hypothesis is created.

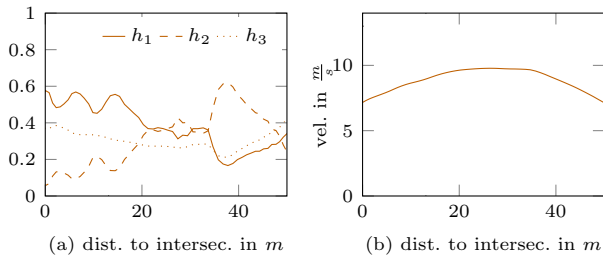## 3. SITUATION RECOGNITION & SITUATION HYPOTHESES SELECTION

Fig. 3. (a) shows the probability of possible hypotheses (h_1(left; right(free drive)), h_2(left; straight(free drive), h_3(left; straight(yield))) dependent on the distance of the affecting vehicle to the intersection. The vehicle actually performs a right turn. (b) shows the corresponding longitudinal velocity profile.

From (8) we see that in order to reliably asses traffic scenes it is necessary to predict future state vectors $\hat{\mathbf{x}}_{t+1:t+s}$ of traffic participants several seconds into the future. However, inner-city traffic scenes exhibit a high variability and complexity, due to the number of possible occurring scene entities and their interactions, which leads to an overwhelming number of necessary predictions. Therefore, we propose to decompose traffic scenes into discrete situations, as proposed in section 2, with similar occurring spatiotemporal trajectory patterns of interacting scene entities forming a discrete prototypical situation. At the same time, we focus on keeping the number of simultaneously considered interacting traffic participants per situation as low as possible. Situations allow to efficiently partition complex, unseen traffic scenes into patterns with limited interactions and predict *situation-specific* future state vector sequences $\hat{\mathbf{x}}_{t+1:t+s}(\mathbf{x}_t, h_t)$.

3.1 Hypothesis Generation and Validation

Based on the evidence of a traffic scene $\mathbf{x}_t$, comprising infrastructure information, dynamic as well as static scene entities, usually a large set $\mathcal{H}$ of situation hypotheses

h_t applies. Each hypothesis consists of one possible path combination for simultaneously considered scene entities (non ego-vehicles are referred to as affecting entities) Additionally, each affecting entity's path is associated with a characteristic *dynamic behavior pattern* (e.g. differing velocity profiles). Typical patterns comprise e.g. giving right of way, driving behind a vehicle, stopping at a traffic light, etc.

The generation process for hypotheses h_t is exemplarily presented focusing on bilateral situations. The hypotheses generation can be divided into three steps, as illustrated in Figure 2, comprising entity grouping, path combinations and dynamic behavior patterns, to arrive at the full set of situation hypotheses $\mathcal{H}$.

To be able to deal with uncertainties, caused by imperfect sensor perception, unobservable variables (e. g. driving intention, style, . . .) and insufficient prediction capabilities, we propose a probabilistic situation hypotheses validation, resulting in a belief $P(h_t|\mathbf{x}_t)$ for each situation hypothesis, as introduced in (3).

For the calculation of the situation hypothesis probability, we use probabilistic classifier methods like proposed in Klingelschmitt et al. (2014). These are fed with different situation indicators based on situation-dependent context information extracted from $\mathbf{x}_t$, which quantify the matches between the entities states with their expected paths and spatiotemporal behavior patterns. The result is $P(h_t|\mathbf{x}_t)$, the probability that a situation h_t will apply to the driving patterns during an upcoming time interval.

Figure 3 shows the result of an exemplary situation hypotheses validation performed on a real-world scenario similar to the one shown in Figure 2 (a), except that the ego-vehicle is planning to make a left turn. In this case, situation hypotheses resulting from the pairwise combination of the ego-vehicle with the orange vehicle are evaluated.

3.2 Hypothesis Selection

Depending on the complexity of the encountered infrastructure and present scene entities, the set of instantiated
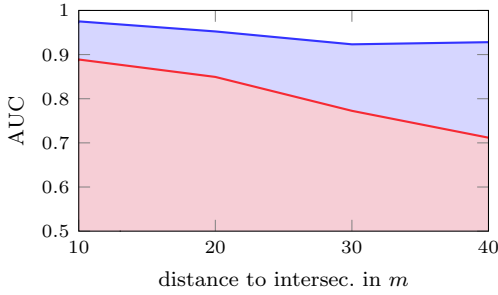
Fig. 4. The AUC curves are based on ROC curves created by adapting the threshold γ for our proposed selection scheme (9) (blue) and a strictly belief-based hypotheses selection ($\gamma < P(h_t|\mathbf{x}_t)$) (red). The *true positive* and *false positive rates* are based on the number of selected situation hypotheses compared to the actually encountered *relevant* situation hypotheses. The data used for the shown quantitative evaluation is obtained from a realistic traffic simulator. A detailed real-world example can be found in Klingelschmitt et al. (2015).

situation hypotheses increases combinatorially. This leads to two main disadvantages. Firstly, the computational costs for predicting and evaluating all hypotheses $h_t \in \mathcal{H}$ several seconds into the future get concomitantly high. Secondly, subsequent risk assessment techniques and behavior planning algorithms also suffer from the amount of hypotheses taken into account. Therefore, we propose a beforehand situation hypotheses selection scheme, with a subsequent concentration on those situations that are relevant for the ego-car's behavior.

The selection is based on combining the situation-specific risk $r(t + s, \mathbf{x}_t, h_t)$ from eq. (8) with the hypothesis belief $P(h_t|\mathbf{x}_t)$ from the validation step in section 3.1 in order to assess if the particular hypothesis h_t needs to be further investigated by subsequent systems. A situation hypothesis is selected, and thus added to the *set of relevant situation hypotheses* $\mathcal{H}'$, if the joint situation-specific risk and hypothesis belief exceed a threshold γ

$$\gamma < r(t + s, \mathbf{x}_t, h_t)P(h_t|\mathbf{x}_t). \quad (9)$$

Since $r(t + s, \mathbf{x}_t, h_t)$ is not yet known at this point and only calculated afterwards as explained in section 2 for the selected situation hypotheses, we proposed to learn situation-specific regression models M_h that estimate expected situation-specific risks from empirical data, as introduced in Klingelschmitt et al. (2015). In order to make conservative and robust estimations, we estimate the situation-specific risk from (9) by using the maximum measured situation-specific risk within the considered time interval $t' \in [t, t+s']$. Hence, we train our situation-specific risk regression models to estimate

$$M_h(\mathbf{x}_t) \sim \max_{s'} r(t + s', \mathbf{x}_t, h_t). $$

Using this approach, the number of superfluously inspected hypotheses can be drastically reduced, as shown by the AUC (**A**rea **U**nder the **C**urve) plots in Figure 4.

4. GENERALIZED PREDICTIVE RISK ESTIMATION

4.1 Predictive Risk Maps

Once we have selected a suitable subset of relevant situation hypotheses which apply to the current ego-car's
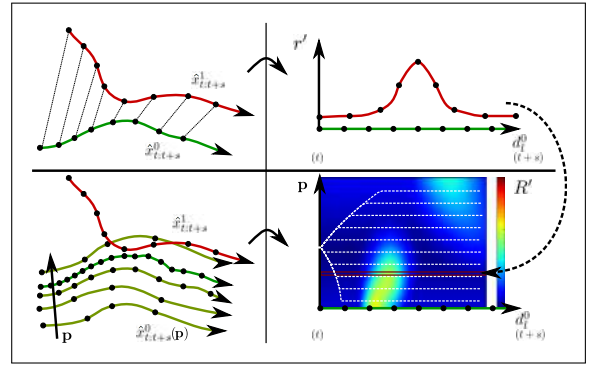

Fig. 5. Predictive Risk Map - Top: evaluation of risk (top right) based on predicted ego car (green) and other car (red) trajectories (top, left) - Bottom: Generation of predictive risk map (bottom, right) based on risk evaluation of a variation of ego car trajectories and other car trajectory (bottom, left).

driving context, the general target of our system is to plan the ego car's future behavior (here future velocity profile) to be safe and of high utility. For this purpose we have to evaluate possible future behavior alternatives in terms of risk and utility. In a first step we concentrate on the behavior evaluation of a single situation. This can be done by building so called Predictive Risk Maps, introduced by Damerow and Eggert (2014), which indicate how risky a certain behavior will be in the future. The trajectory prediction of one situation provides one predicted prototypical trajectory for each involved entity, here $\hat{\mathbf{x}}^0_{t:t+s}$ for the ego and $\hat{\mathbf{x}}^1_{t:t+s}$ for another car. We can now evaluate the risk by comparing the ego car's and one other car's trajectory pairwise at the same moment in predicted time using the situation dependent risk function (8). For illustrative purposes we use the risk over longitudinal distance d^0_l instead of future time s, as we can equivalently write $r'(d^0_l, \mathbf{x}_t, h_t) = r(t + s(d^0_l), \mathbf{x}_t, h_t)$.

As a result we gain a measure for future risk, illustrated in Fig. 5 (top). If we now build a variation of ego car trajectories $\hat{\mathbf{x}}^0_{t:t+s}(\mathbf{x}_t, h_t, p)$ using a variation parameter p and evaluate the risk for each variation, we gather a predictive risk map $R(t + s, \hat{\mathbf{x}}^0_{t+s}(\mathbf{x}_t, h_t, p), \mathbf{x}_t, h_t)$, or

$$R'(d^0_l, \hat{\mathbf{x}}^0_d(\mathbf{x}_t, h_t, p), \mathbf{x}_t, h_t), \quad (10)$$

as shown in Fig. 5 (bottom).

Here we vary only the ego car longitudinal velocity $v^0_l(\mathbf{x}_t, h_t, v^0_{l,target})$ using different target velocities $v^0_{l,target}$ and incorporate dynamic constraints in terms of maximal acceleration/deceleration indicated by the dashed white trajectories in Fig. 5 bottom right. As a result we arrive at a predictive risk map in the (d^0_l, v^0_l)-plane for a fixed initial state $\mathbf{x}_t$ and one situation h_t, as $R'(d^0_l, v^0_l)$ [3] (in the following we omit constant parameters in case they are not necessary).

We now search for low-risk paths across the risk map. These will vary from the predicted trajectories $\hat{\mathbf{x}}^0_d(\mathbf{x}_t, h_t, p)$ used for building the risk map (e.g. dashed white lines in Fig. 5 bottom right), leading to distortions in the risk map. For small deviations from the original trajectories,

---

[3] Remark however that risk maps which depend on more complex ego-car behavior parameterization, as e.g. for lateral control, can be treated similarly.
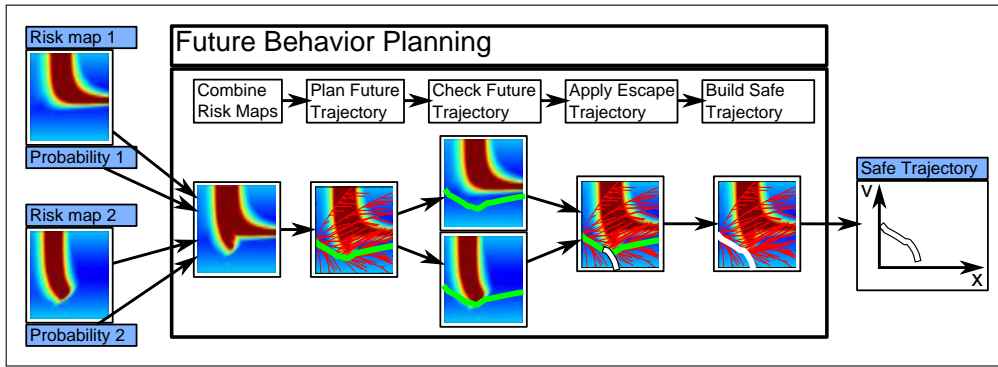
Fig. 6. Planning of safe and efficient future behavior: Scenario with 2 active situations with different probabilities, generating 2 risk maps. Both are then weighted with their situation occurrence probability and combined into one risk map, which is then used to plan the future behavior. The resulting trajectory is then checked for risk threshold violations in each situation and escape trajectories are applied. As a result we get an efficient safe trajectory by using the planned future trajectory with the earliest necessary escape trajectory.
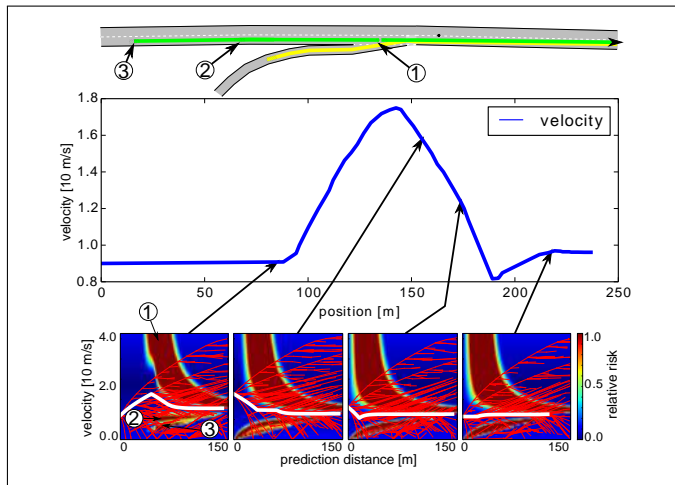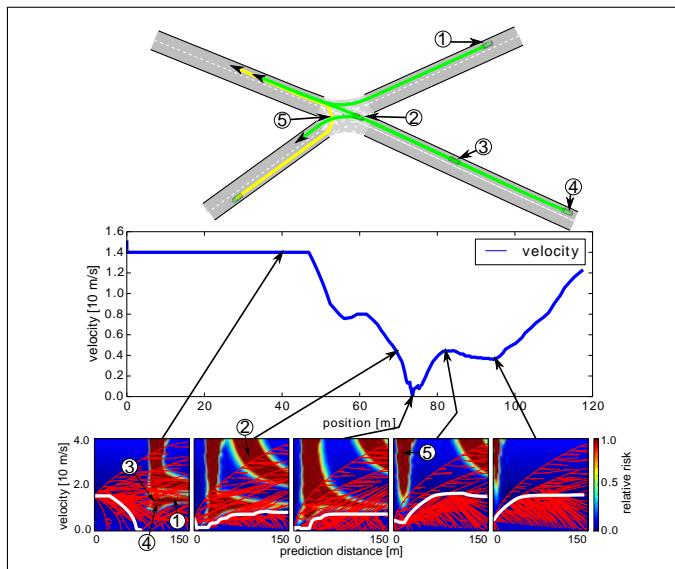

Fig. 7. Highway Accessing.

Fig. 8. Complex Turning Behavior: other cars as risk sources (1-4), curve as risk source (5).

however, the risk map topology does not vary substantially and can be used for planning.

4.2 Safe Trajectory Planning in Dynamic Environments

With the predictive risk maps $R'(d_l^0, v_l^0)$ for a certain situation we can now plan the best possible future behavior using e.g. a sampling based trajectory planner such as RRT*. The RRT* is an extension to the general RRT (Rapidly exploring Random Tree) enabling the algorithm to converge to the globally optimal solution minimizing a given cost function. As presented by Damerow and Eggert (2015) we use the algorithm to plan the ego car's future trajectory minimizing the overall costs as a combination of risk and utility normalized by the ego car's driven distance,

$$\mathrm{Cost}(d_l^0, v_l^0) = \frac{1}{d_l^0} \int_0^{d_l^0} [R'(d_l, v_l^0) + \mathrm{TC}(d_l, v_l^0)]\mathrm{d}d_l \ , (11)$$

with the utility / travel costs TC. We employ a cost function which is linearly increasing with the deviation of the ego car's velocity v_l^0 from the desired velocity $v_{l,des}^0$. TC_0 and m define the minimal travel costs and slope of the cost function.

$$\mathrm{TC}(d_l^0, v_l^0) = \mathrm{TC}_0 + m \, |v_{l,des}^0 - v_l^0| \ . \tag{12}$$

The simulation results in Figs. 7 and 8 show, that this approach can be applied to a wide range of different scenarios, starting from highway scenarios with multiple traffic participants (e.g. Fig. 7) up to complex inner city scenarios (e.g. turning left at an unmanaged intersection with multiple other traffic participants involved (see Fig. 8). The turning scenario illustrates that our approach is also able to handle multiple types of risk, here additionally the risk for loosing control in curves due to high lateral acceleration, besides collision risks caused by several other dynamic objects.

4.3 Safe Trajectory Planning under Multiple Situations with Uncertainty

Until now we concentrated on a single, although complex, situation to plan the future behavior, using only one predicted spatiotemporal trajectory for each involved traffic participant. However, the situation classification and selection steps described in section 3.1 are in general not able to provide the one and only occurring situation, but a selection of situation hypotheses h_t. We additionally obtain the occurrence probability $P(h_t|\mathbf{x}_t)$ for each selected

(a) **(straight;left(yield))** Other car (purple) stopping to give way for the ego car (green).

(b) **(straight;left(free))** Other car not stopping due to overlooking the ego car.

(c) Driven velocity profiles.

(d) Situation occurrence probabilities $P(h_t|\mathbf{x}_t)$.

(e) Combined predictive risk maps timeline $t = [0, 2, 4, 6]s$ including planned future trajectory (green) and safe future trajectory (white).

(f) Situation-dependent unweighted predictive risk maps and planned future trajectory including risk threshold violations (white arrow). "other stopping" situation (top) and "other not stopping" situation (bottom).

(g) Comparison of velocity profiles. Check indicates correct situation classification, flash indicates wrong situation classification
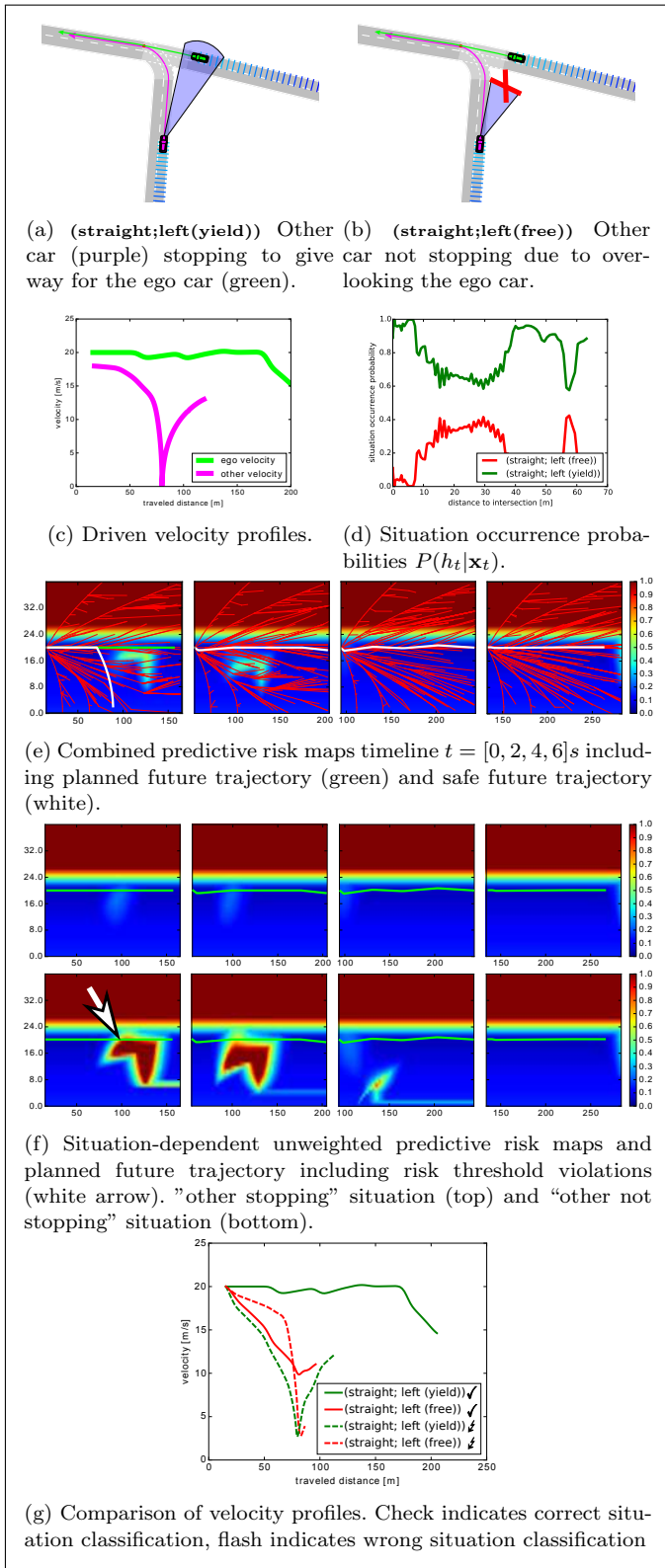
Fig. 9. T-Intersection with uncertainty if other car is giving way.

situation and, by the following trajectory prediction step of each situation, one predicted trajectory for each involved entity. The target is now to find a future behavior which is of low risk and high utility in all hypothetical situations, and especially in the situation that will finally occur. The risk evaluation step generates one predictive risk map per

situation using the situation dependent predicted trajectories $\hat{\mathbf{x}}_{t:t+s}(\mathbf{x}_t, h_t)$.

The behavior planning step, consisting of 5 sub-steps, is shown in detail in Fig. 6. It is based on the concept of planning the future behavior with high utility for the most probable situation and additionally keeping an always safe, but possibly inefficient "plan b" for the other situations. By following these steps, we obtain a future behavior which is of high utility for a confident situation classification, but still safe for the case of an unconfident or even wrong situation classification. For this purpose, we first join the predictive risk maps of all possible situation hypotheses in a combined predictive risk map, according to (7) and (8).

$$R'(d_l^0, v_l^0) = \sum_{h_t \in \mathcal{H}'} R'(v_l^0, d_l^0, h_t) \frac{P(h_t|\mathbf{x}_t)}{\max\limits_{h_t' \in \mathcal{H}'}(P(h_t'|\mathbf{x}_t))}. \quad (13)$$

This has the desired effect that the most likely situation is fully taken into account for behavior planning, whereas the other, less likely, situations are still taken into account, but weighted with $P(h_t|x_t)/\max_{h_t'}(P(h_t'|x_t)) \leq 1$. This results in a future behavior that mostly adapts to the best behavior for the most likely situation, but smoothly incorporates less likely situations. A confident situation classification would provide high probability only for one situation and low probability for the other situations. In this case the behavior adapts almost only to the best behavior of the most probable situation. In case of an unconfident situation classification, there are several situations with similar probability, and the resulting behavior would take risk of all those situations similarly into account.

Still we can not ensure an always safe behavior for the case that an unlikely situation suddenly kicks-in. Although the risk of this unlikely situation was partially taken into account and the resulting behavior averts this situation's risk, this might not be sufficient to ensure a safe behavior for this situation.

Thus in a further step we check the planned future trajectory for a risk threshold violation on each situation's risk map. In case of a threshold violation we then apply an escape trajectory (e.g. emergency braking) as late as possible, but as early as necessary to safeguard the situation for the case it actually kicks in. The finally executed safe trajectory consists of two parts, the trajectory of high utility planned using the combined risk map, followed by a possibly necessary escape trajectory. In general / in case of a confident situation classification, situations with low probability and high risk drop even further in probability and are finally discarded by the situation classification step as explained in section 3.2, or drop in risk, as the entities act in a risk aversive manner. As we reevaluate and replan from time to time the escape trajectory will usually never be executed. Only if a risky situation does not drop in risk and/or occurrence probability this escape trajectory will be executed to keep the overall situation safe.

In Fig. 9 we present a scenario, where a car approaches a T-intersection and plans to turn left onto the ego car's way. We analyze how our approach copes with the two hypothetical alternatives that (a) the other car yields to the ego car and (b) the other car violates the left-yields-to-right-rule and drives through. The most common scenario - the other car yielding way of right - is analyzed in detail

using the generalized predictive risk estimation approach. In this case, the situation classification (d) results in a high probability for the correct situation (a) and a low probability for situation (b). The predictive risk maps in (f) for the two situations are calculated and combined (wheighted by their occurrence probabilities) into the overall risk map (e), which is then used by the RRT* planner to calculate the desired future behavior (green line). This is then checked and safeguarded with possibly necessary escape trajectories (white line). The resulting ego-velocity profile (c) for this scenario shows a behavior of low risk and high utility (not significantly slowing down). In Fig. 9 (g), we compare different alternative cases, where the situation classification provides a false or correct classification results for the two situations (that the other car stops or does not stop). A wrong situation classifications deteriorates the resulting trajectories leading to an emergency braking maneuver, however they still are within the low-risk bounds of operation.

Confirmed by the simulation results the approach enables to plan safe and efficient trajectories for the case of a confident and correct situation classification. With lower situation classification confidence we get a less efficient, but still safe future behavior. This holds even for the case that the situation classification favors the wrong situation.

5. SUMMARY

We proposed a general approach for predictive risk estimation and behavior planning in dynamic environments that can be applied to several different scenarios comprising a mixture of risks such as e.g. longitudinal collision risks, risks of passing nearby without collision, risks at intersections and highway entrances and risks in curves.

The predictive risk approach allows to incorporate the inherent uncertainty that is involved when dealing with long-term trajectory predictions and noisy sensor measurements. Risks that are still further away in the future appear broader and more delocalized in space and time, increasing and sharpening as they become more imminent. The results show that different types of risk can be integrated within a single, generalizing model which additionally scales with increasing complexity. The same model results in simulated smooth and low-risk driving trajectories for such diverse situations as unmanaged intersections, lane entrances and lane changes. In the inspected situations with a simulated driver, the resulting behavior mimics that of a "foresighted" driver who is aware of the upcoming risks and reacts proactivley to avoid them. For real-world operation, the approach requires sensor-based estimations of the other traffic participants positions and velocities as well as of the road structure, which will be available in the not-so distant ADAS future.

After the desired types of risks have been selected and parameterized, we can apply the same type of estimation as a measurement for the quality of a performed driving action. E.g., the risk along a driving route can be measured with and without a certain new ADAS function, allowing for an efficient continuous quantification and validation of new ADAS functions by risk in conditions where conventional approaches like TTC are insufficient.

REFERENCES

Althoff, M., Stursberg, O., and Buss, M. (2009). Model-based probabilistic collision detection in autonomous driving. *IEEE Trans. on Int. Transp. Sys.*, 10, 299–310.

Chinea, A. and Parent, M. (2007). Risk assessment algorithms based on recursive neural networks. In *The 2007 International Joint Conference on Neural Networks (IJCNN)*, 1434–1440.

Damerow, F. and Eggert, J. (2014). Predictive risk maps. In *ITSC*, 703–710. IEEE.

Damerow, F. and Eggert, J. (2015). Balancing risk against utility: Behavior planning using predictive risk maps. In *IV*, in press. IEEE.

Eggert, J. (2014). Predictive risk estimation for intelligent adas functions. In *ITSC*, 711–718. IEEE.

Eggert, J., Damerow, F., and Klingelschmitt, S. (2015). The foresighted driver model. In *IV*. IEEE.

Hall, D. and Llinas, J. (1997). An introduction to multisensor data fusion. In *Proc. of the IEEE*, volume 85, 6–23.

Hillenbrand, J., Spieker, A.M., and Kroschel, K. (2006). A multilevel collision mitigation approach - its situation assessment, decision making, and performance tradeoffs. *IEEE Trans. on Int. Transp. Sys.*, 7(4), 528–540.

Käfer, E., Hermes, C., Wöhler, C., and Kummert, F. (2010). Recognition and prediction of situations in urban traffic scenarios. In *ICPR*, 4234 – 4237. IEEE.

Klingelschmitt, S., Damerow, F., and Eggert, J. (2015). Managing the complexity of inner-city scenes: An efficient situation hypotheses selection scheme. In *IV*, 388–393.

Klingelschmitt, S., Platho, M., Gross, H.M., Willert, V., and Eggert, J. (2014). Combining behavior and situation information for reliably estimating multiple intentions. In *IV*, 388–393. doi:10.1109/IVS.2014.6856552.

Lefèvre, S., Laugier, C., and Ibañez-Guzmán, J. (2013). Intention-aware risk estimation for general traffic situations, and application to intersection safety. Research Report RR-8379.

Lefèvre, S., Vasquez, D., and Laugier, C. (2014). A survey on motion prediction and risk assessment for intelligent vehicles. *Robomech Journal*, 1(1).

Rodemerk, C., Habenicht, S., Weitzel, A., Winner, H., and Schmitt, T. (2012). Development of a general criticality criterion for the risk estimation of driving situations and its application to a maneuver-based lane change assistance system. In *IV*, 264–269. IEEE.

Salim, F., Loke, S., Rakotonirainy, A., Srinivasan, B., and Krishnaswamy, S. (2007). Collision pattern modeling and real-time collision detection at road intersections. In *ITSC*, 161–166. IEEE.

Schreier, M., Willert, V., and Adamy, J. (2014). Bayesian, maneuver-based, long-term trajectory prediction and criticality assessment for driver assistance systems. In *ITSC*, 703–710. IEEE.

Shladover, S.E. (2009). Automated driving in progress and prospects. In *ITSC*. IEEE.

TRACE project (2008). Accident causation and pre-accidental driving situations - in-depth accident causation analysis. In *Deliverable D2.2.*

van der Horst, A. (1991). *Vision in Vehicles III*, chapter Time-to-Collision as a cue for decision making in braking, 19–26. Elsevier.